ARTICLE

Experimental Study of Premixed Stoichiometric Ethylene/Oxygen/Argon Flame

Qing Zhang[a], Yu-yang Li[b], Zhen-yu Tian[b], Tai-chang Zhang[b], Jing Wang[b], Fei Qi[b]*

a. School of Mathematics and Physics, Anhui University of Technology, Ma'anshan 243002, China
b. National Synchrotron Radiation Laboratory, University of Science and Technology of China, Hefei 230029, China

(Dated: Received on July 6, 2006; Accepted on September 4, 2006)

A comprehensive experimental study of the premixed ethylene/oxygen/argon flame at 2.667 kPa with a stoichiometric equivalence ratio (ϕ=1) was performed with the tunable synchrotron photoionization and molecular-beam sampling mass spectrometry techniques. The isomers of most observed species in the flame were unambiguously identified by measurements of the photoionization efficiency spectra, e.g. C_3H_4, C_2H_4O and C_4H_4. The mole fraction profiles of species up to C_7H_8 were measured by scanning the burner position at the selected photon energies near ionization thresholds, and the flame temperature profile was obtained by using Pt/Pt-13%Rh thermocouple. Compared with the previous studies, a lot of new flame species: C_3H_2, C_3H_3, C_3H_5, C_2H_6O, C_4H_2, C_4H_4, C_4H_6, C_3H_4O, C_3H_6O, C_3H_8O, C_5H_6, C_4H_8O and C_7H_8, were observed. A series of free radicals in the flame are detected to be CH_3, C_2H_3, C_2H_5, HCO, C_3H_3 and C_3H_5. Based on the experimental work, a reduced reaction mechanism was developed including 40 species and 223 reactions. Modeling and measurements agree well for the major species and most intermediates. A detailed kinetic model is desired for this flame.

Key words: Premixed ethylene/oxygen flame, Tunable synchrotron photoionization, Reaction mechanism

I. INTRODUCTION

Ethylene flame is an important system in combustion chemistry, which is used extensively in studies of flame structure and propagation, shock tube ignition and detonation. Ethylene is a major component of commonly used fuels and is thought to be the key intermediate in the oxidation of alkanes [1,2] and higher alkenes, which is formed by fuel decomposition processes in early flame stages or in zones of high pyrolysis rate. It's one of the simplest unsaturated hydrocarbons and can easily undergo O atom addition to the double bond, resulting in the formation of oxygenated species such as aldehydes and oxiranes. Furthermore, formation of ethylene and its subsequent reactions to acetylenic derivatives are believed to play important roles in the kinetics of gas-phase soot formation.

A lot of experimental investigations on ethylene flames were performed under different conditions previously. Most researchers studied C_2H_4 flames with molecular-beam mass spectrometry (MBMS), for example Peeters and Mahnen [3], Peeters and Vinckier [4], and Homann *et al.* [5]. Recently, Bhargava and Westmoreland studied ethylene flames in detail with MBMS and electron-impacted ionization (EI) under lean (ϕ=0.75) and rich (ϕ=1.90) conditions [6,7]. On the other hand, Harris *et al.* and Cool *et al.* have measured some flame species in ethylene flames with species-specific laser-based techniques like laser-induced fluorescence (LIF) and resonance-enhanced multiphoton ionization (REMPI) [8,9]. However, it is hard to draw a complete picture for ethylene flame because there are some limitations for the above methods in detecting flame species and identifying isomers [10,11].

Modeling is a key step in understanding flame chemistry. Westbrook *et al.* developed a simple mechanism for high temperature pyrolysis and oxidation of ethylene [12], and Cathonnet *et al.* carried out kinetic study of ethylene oxidation in tubular reactor [13]. In the last decade, some groups, including Lindstedt and Skevis [14], Richter and Howard [15], and Carriere *et al.* [16] have developed kinetic models of low-pressure ethylene flames, all based on the experimental data of Bhargava and Westmoreland [6,7].

In this work, a low-pressure premixed $C_2H_4/O_2/Ar$ flame (ϕ=1.0) is studied using the synchrotron photoionization and MBMS techniques. To our knowledge, the ethylene flame with the stoichiometric equivalence ratio has not been studied yet. The high resolution of photoionization mass spectrometry (PIMS) allows unambiguous measurement of flame species and isomer-specific detection of intermediates, while the single-photon process can avoid the influence of photoionization fragments. Measurements of concentration profiles and photoionization efficiency (PIE) spectra for species are performed. The comprehensive experimental data are useful to develop the kinetic model of the ethylene flame and extend the knowledge of hydrocarbon combustion processes. Besides, mole fraction prediction of major species and intermediates is also accomplished in

*Author to whom correspondence should be addressed. E-mail: fqi@ustc.edu.cn

this work, using a reduced reaction mechanism.

II. EXPERIMENTAL METHOD

This work was carried out at the flame endstation of National Synchrotron Radiation Laboratory in Hefei, China. The instrument has been reported elsewhere [17]. In brief, a low-pressure laminar premixed flame stabilized on a 6.0 cm diameter flat burner is sampled through a quartz nozzle with an orifice diameter of ~500 μm in the tip. The sampled gas forms a molecular beam, which is skimmed and then passes into a differentially pumped ionization region where it is crossed by the tunable synchrotron light. The photoions are collected and analyzed by a home-made reflectron time-of-flight mass spectrometer (RTOFMS) [18]. Movement of the burner towards or away from the quartz nozzle allows mass spectrum to be taken at different position in the flame. A LiF window is used to eliminate higher-order harmonic radiation when the wavelength is longer than 105 nm.

The $C_2H_4/O_2/30\%$Ar flame (ϕ=1.0, C/O=0.33) at a pressure of 2.667 kPa (20 Torr) was used for this study. The flow rates for C_2H_4, O_2 and Ar were 0.45, 1.35 and 0.77 L/min (SLM), respectively. The mass flow rate was 0.0023 g/cm^{2}s with a cold (300 K) flow velocity of 57.57 cm/s. The temperature profile was measured by using Pt/Pt-13%Rh thermocouple, 0.076 μm in diameter, coated with Y_2O_3-BeO anti-catalytic ceramic to avoid catalytic effects [19]. The radiative heat losses has been considered and calibrated for the temperature profile. The thermocouple was placed 15 mm upstream of the sampling cone. The integrated ion signals for a given mass are normalized by photon flux, and plotted as a function of the photon energy, which then yield the PIE spectra containing precise information of the ionization energies (IEs) of corresponding species. Some PIE spectra taken at 4.0 mm above the burner surface are chosen for distinguishing isomers. Considering the cool effect of molecular beam [20], the experimental error of the measured *IE* is within 0.05 eV. In order to avoid fragmentation and keep near-threshold ionization, we scanned the burner position at some selected photon energies: 16.53, 11.70, 11.00, 10.00 and 9.50 eV. The mole fractions of the species are derived according to the method described by Cool *et al.* [21]. In this work, no correction is made to the concentration profiles to compensate for the fact that the sampling cone draws from a flame region extending about several nozzle diameters ahead of the cone [22,23]. The mole fractions have an uncertainty of ±25% for the stable intermediates, and a factor of 2 for radicals.

III. RESULTS

Mole fraction profiles of major species C_2H_4, O_2, Ar, H_2, H_2O, CO and CO_2 are shown in Fig.1, along with

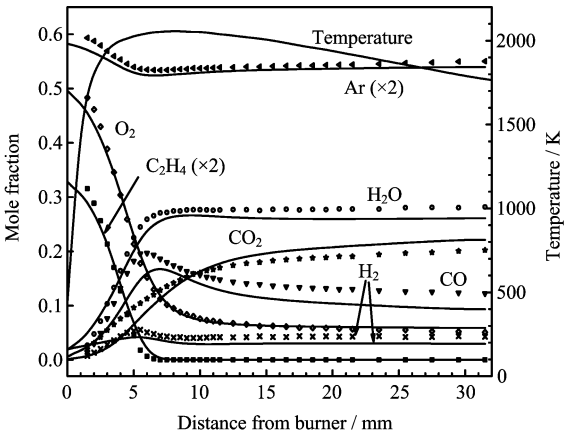

FIG. 1 Mole fraction profiles of the major species (e.g. Ar, C_2H_4, O_2, CO, CO_2, H_2 and H_2O) and the flame temperature profile. Symbols are experimental data and curves for calculated profiles.

the calibrated temperature profile. The fuel ethylene is fully consumed by 7 mm, while the mole fraction of oxygen drops to be 0.1 at this position. That means the reaction zone is from 0 to 7 mm where H_2 and CO rise sharply to maximum mole fractions of 5.5×10^{-2} and 0.20. The flame region after 7 mm could be recognized as a post-flame zone. In this region, CO and O_2 will keep falling and form CO_2. The final mole fractions of H_2, H_2O, CO, CO_2 and remaining O_2 are 4.3×10^{-2}, 0.28, 0.12, 0.20 and 0.05, respectively. The mole fraction of Ar, which is used as a basis for calculating instrumental sampling functions, decreases quickly from 0.30 in the fresh gas to 0.267 in the reaction zone and climbs slowly to 0.275 in the post flame. A maximum temperature of 2057±100 K is observed at 10.0 mm. The isomer-specific intermediates measured in this flame are listed in Table I along with their *IE*s, maximum mole fractions and positions. The *IE*s are derived from the PIE spectra taken at the burner position of 4.0 mm above the burner surface. The mole fraction profiles of flame intermediates from C_1- to C_7-species are shown in Fig.2 and Fig.3 as following. To simplify the figures, mole fractions of isomers will not be given separately and the total mole fraction for each mass is shown instead. The mole fractions of H, O and OH radicals are not provided because their ionization energies are beyond the cutoff of the LiF window.

The mole fractions of the observed C_1- and C_2-hydrocarbons are shown in Fig.2(a). The smallest hydrocarbon species detected is methyl radical (CH_3) with a maximum mole fraction of 1.98×10^{-3}. Two C_2-hydrocarbons C_2H_2 and C_2H_3 are detected with the maximum mole fractions of 1.10×10^{-2} and 7.03×10^{-6}. Previous studies indicated that vinyl is the major product of ethylene destruction and its dominant product is acetylene which will then be converted rapidly to CO and CO_2 [6,7]. CH, CH_2 and C_2H are not observed in

ISSN 1003-7713/DOI:10.1360/cjcp2006.19(5).379.7

TABLE I List of intermediates examined and measured along with their *IE*s, maximum mole fractions (X_{max}) and positions

Mass	Formula	Species name	*IE*/eV		Concentration	
			Literature[24]	Measured(±0.05)	Position/mm	X_{max}
15	CH_3	Methyl radical	9.84	9.84	4.0	1.98×10^{-3}
26	C_2H_2	Acetylene	11.40	11.40	5.0	1.10×10^{-2}
27	C_2H_3	Vinyl radical	8.59	8.60	5.0	7.03×10^{-6}
29	HCO	Formyl radical	8.12	8.20	2.0	3.54×10^{-5}
	C_2H_5	Ethyl radical	8.12	8.20	2.0	3.54×10^{-5}
30	H_2CO	Formaldehyde	10.88	10.88	3.0	5.34×10^{-3}
32	CH_3OH	Methyl alcohol	10.84	10.85	3.0	3.36×10^{-4}
38	C_3H_2	Propadienylidene	10.43	10.44	5.0	7.41×10^{-6}
39	C_3H_3	Propargylradical	8.67	8.69	5.0	3.37×10^{-5}
40	C_3H_4	Propyne	10.36	10.33	4.5	1.03×10^{-4}
	C_3H_4	Allene	9.692	9.69	3.5	3.51×10^{-5}
41	C_3H_5	Allyl radical	8.18[a]	8.14	4.5	1.88×10^{-5}
42	C_2H_2O	Ketene	9.62	9.63	4.5	1.24×10^{-3}
43	C_2H_3O	Vinyloxy radical	10.85	10.83	3.0	6.38×10^{-5}
44	C_2H_4O	Acetaldehyde	10.23	10.25	2.5	9.38×10^{-4}
	C_2H_4O	Ethenol	9.33	9.32	3.5	3.73×10^{-5}
46	C_2H_6O	Dimethyl ether	10.03	10.08	2.5	1.58×10^{-4}
50	C_4H_2	1,3-butadiyne (diacetylene)	10.17	10.16	5.0	1.90×10^{-5}
52	C_4H_4	1-buten-3-yne (vinylacetylene)	9.58	9.59	4.5	2.83×10^{-5}
	C_4H_4	1,2,3-butatriene	9.25	9.22	3.0	$<1.00\times10^{-6}$
54	C_4H_6	1,3-butadiene	9.07	9.08	4.0	5.56×10^{-5}
56	C_3H_4O	Methylketene	8.95	8.92	3.5	2.61×10^{-5}
58	C_3H_6O	Acetone	9.70	9.65	3.0	1.79×10^{-5}
60	C_3H_8O	Methyl ethyl ether	9.72	9.78	2.0	2.56×10^{-5}
66	C_5H_6	1,3-cyclopentadiene	8.57	8.60	4.5	5.38×10^{-6}
72	C_4H_8O	2-butanone	9.52	9.56	2.0	4.92×10^{-6}
78	C_6H_6	Benzene	9.24	9.23	4.5	1.26×10^{-6}
92	C_7H_8	Toluene	8.83	8.84	4.0	8.16×10^{-6}

[a] Ref.[38]

this flame, which is in agreement with Bhargava's work [6]. For mass 29, there is only one onset at 8.20±0.05 eV on the PIE spectra. Two radicals HCO (*IE*=8.12 eV [24]) and C_2H_5 (*IE*=8.117 eV [24]) are both considered to be existing in this flame. The maximum mole fraction of mass 29 is located at about 2 mm (the preflame region), which suggests that the oxygenated radical (HCO) is dominant for mass 29.

The mole fractions of C_1 and C_2-oxygenated species are displayed in Fig.2(b). H_2CO is principally produced from methyl oxidation [25], reaching the maximum of 5.34×10^{-3} at 4.0 mm. As mentioned above, HCO coexists with C_2H_5 and the mixture has a maximum mole fraction of 3.54×10^{-5}. Its major formation channels contain O addition to ethylene and H abstraction from H_2CO. Methanol has a peak value of 3.36×10^{-4} at 3.0 mm and is thought to be formed from the radical recombination of CH_3 and OH [26]. For mass 42, there are two possible isomers ketene (*IE*=9.617 eV [24]) and propylene (*IE*=9.73 eV [24]). Bhargava and Westmoreland did not distinguish these two species because the minor difference between their *IE*s is a real challenge to the energy resolution of EIMS, and they chose ketene to be the major species after the preliminary modeling [6]. However, ketene and propylene can be clearly distinguished by our synchrotron PIMS. In this flame, ketene is detected to be the dominant one because only one onset is observed at 9.63±0.05 eV on the PIE spectra shown in Fig.4, which has a maximum mole fraction of 1.24×10^{-3} at 4.5 mm. The signal of C_2H_3O is assigned to the vinyloxy radical. Its mole fraction has been corrected for isotopic contribution from ketene and the maximum is 6.38×10^{-5}. PIE spectra of mass 44 is displayed in Fig.5. Two onsets of 10.25±0.05 and 9.32±0.05 eV are clearly observed, which indicates that mass 44 consists of acetaldehyde (*IE*=10.23 eV

ISSN 1003-7713/DOI:10.1360/cjcp2006.19(5).379.7

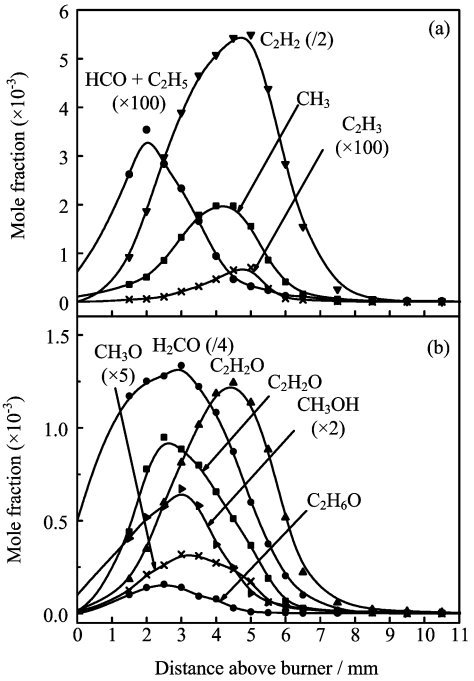

FIG. 2 Mole fraction profiles for (a) C_1- and C_2-hydrocarbons, (b) C_1 and C_2-oxygenatad species. Symbols are experimental data with curve extrapolations to guide the eye.

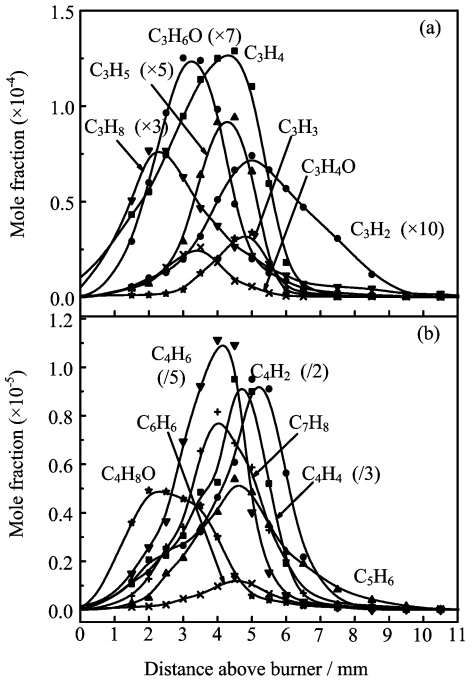

FIG. 3 Mole fraction profiles for (a) C_3-species; (b) C_4 to C_7-species. Symbols are experimental data with curve extrapolations to guide the eye.

[24]) and ethenol (IE=9.33 eV [24]). Acetaldehyde is a toxic pollutant and has a peak value of 9.38×10^{-4}. Its isomer ethenol is recently detected as a common intermediate in hydrocarbon flames [27] with a maximum value of 3.93×10^{-5}. In C_2H_4 flames, the dominant production mechanism of ethenol is the reaction of OH with C_2H_4 [28]. The total maximum mole fraction of C_2H_4O is 9.49×10^{-4} at 2.5 mm. Among the observed C_2-oxygenates, the largest one is C_2H_6O which is assigned to be dimethyl ether and has a maximum mole fraction of 1.58×10^{-4}.

The C_3-species are shown in Fig.3(a). C_3H_2 with an ionization threshold of 10.44±0.05 eV is identified as singlet propadienylidene (IE=10.43 eV [24]) with a maximum mole fraction of 7.41×10^{-6}, and the contributions from triplet propargylene (IE=8.96 eV) and singlet cyclopropenylidene (IE=9.15 eV [27]) are probably negligible. According to Fig.4, the propargyl radical is considered as the mass 39 species and has a maximum mole fraction of 3.37×10^{-5} at 5.0 mm. Modeling [14,15,29] indicates that propargyl can self-combine to form benzene and phenyl [30-32], which is thought to be the rate-limiting step in the formation of polycyclic aromatic hydrocarbons (PAH) and soot [33]. It is the first time to detect propargyl in lean and stoichiometric ethylene flames ($\phi\leq1.0$). Mass 40 is not mentioned in Bhargava's paper, while we detected it as C_3H_4 with a total maximum mole fraction of 1.29×10^{-4} at 3.5 mm. From the PIE spectra shown in Fig.5, two ionization thresholds are measured to be 9.69±0.05 and 10.33±0.05 eV which correspond to the IEs of allene and propyne. The two isomers are both precursors for the propargyl radical and reach the peak values at 3.51×10^{-5} and 1.03×10^{-4}, respectively. The role of allene in benzenoid ring formation mechanism has been studied by Law *et al.* [34], which shows that large allene concentration can lead to great increment of the propargyl radical and benzene contents in ethylene flame. C_3H_5 is the allyl radical with a maximum mole fraction of 1.88×10^{-5}. Three C_3-oxygenated species are observed in this study. C_3H_4O is identified as methylketene with a maximum mole fraction of 2.61×10^{-5}. C_3H_6O is acetone and has a peak value of 1.79×10^{-5}. For mass 60, ethyl methyl ether is the dominant species with a maximum mole fraction of 2.56×10^{-5}. There is no obvious evidence for the existence of propanol in this flame.

The species containing more than four carbon atoms are shown in Fig.3(b). C_4H_2 (1,3-butadiyne) is the smallest C_4-hydrocarbons in this work with a maximum value of 1.90×10^{-5}. On the PIE spectra of mass 52 (C_4H_4), two onsets are observed at 9.22±0.05 and 9.59±0.05 eV corresponding to 1,2,3-butatriene and vinylacetylene, respectively. The total mole fraction is 2.85×10^{-5} at 4.5 mm while vinylacetylene has a maximum mole fraction of 2.83×10^{-5} at the same position. 1,2,3-butatriene has a much lower mole fraction with an estimated peak value of less than 10^{-6}. For C_4H_6, 1,3-butadiene is clearly detected as the dominant species

ISSN 1003-7713/DOI:10.1360/cjcp2006.19(5).379.7

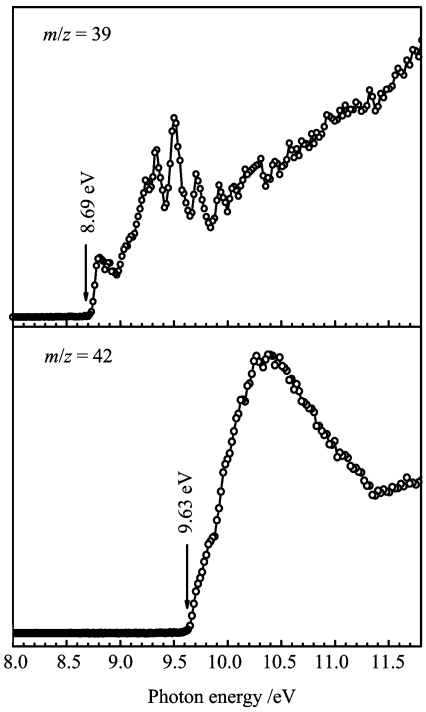

FIG. 4 PIE spectra of mass 39 and 42 along with the measured *IE*s.

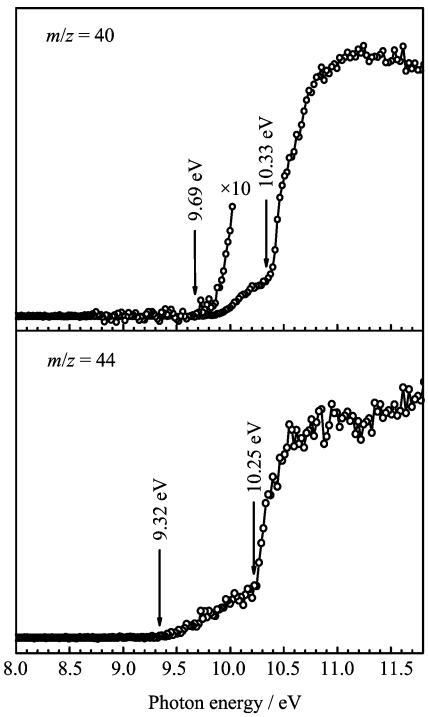

FIG. 5 PIE spectra of mass 40 and 44. There are two onsets for each mass corresponding to different isomers.

with a maximum mole fraction of 5.56×10^{-5} at 4 mm. It is identified as a hazardous air pollutant by the 1990 U.S. Clean Air Act, and its cancer risk potency is 25 times higher than benzene [35]. All the four hydrocarbons are detected in the stoichiometric ethylene flame for the first time. Four species with molecular weights greater than 60 are also shown in this Fig.3. C_5H_6 is identified as 1,3-cyclopentadiene with a maximum mole fraction of 5.38×10^{-6} at 4.5 mm. The mass 72 is identified to be 2-butanone with the peak mole fraction of 4.92×10^{-6} in this flame. For mass 78, benzene is unambiguously detected with a maximum mole fraction of 1.26×10^{-6} at 4.5 mm. And its isomer fulvene has not been observed due to it is low concentration which is in agreement with Bhargava's work [6]. The largest species detected in this flame is toluene, which has a peak value of 8.16×10^{-6} at 4.0 mm. Among these species, 2-butanone and toluene are observed in similar ethylene flames for the first time.

IV. DISCUSSION

A. Modeling major species

A reduced chemical kinetics mechanism has been developed for modeling this flame. This mechanism contains 40 species and 223 elementary reactions. Figure 6 provides a simplified reaction net in this flame. Premixed laminar burner-stabilized flame model of CHEMKIN is used for this work. The calibrated temperature profile is lowered by 100 K to account approximately for the cooling effect of the probe [36,37].

Compared with previous work [15,34], a good performance has been achieved in predicting major species. Figure 1 shows the comparison between experimental and computational profiles. From the figure, predicted mole fraction profiles of the major species are in very good agreement with experimental measurements and the biggest discrepancies within the flame region are in the post-flame zone. The error in predicting CO and

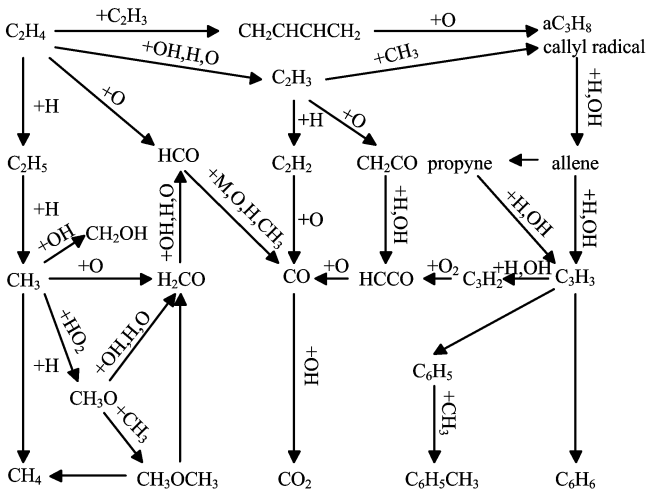

FIG. 6 Simplified reaction pathways for some important ethylene combustion process.

ISSN 1003-7713/DOI:10.1360/cjcp2006.19(5).379.7

CO_2 is probably related to the overprediction of hydroxyl radical in the post-flame zone, which moves the equilibrium of the reaction

$$CO + OH \rightarrow CO_2 + H \quad (1)$$

to the right and leads to the shifts of CO and CO_2 concentrations. Another possible source of error might be the discrepancies of temperature as most key reactions are temperature dependent.

B. Modeling intermediates

Flame intermediates play important roles in fuel destruction and pollutant formation processes. This model predicted more than 30 intermediates observed in this work. Figure 7 shows the predicted and measured mole fractions of the propargyl radical and 1,3-butadiene. The predicted profile of the propargyl radical coincides very well with experimental data. The computed peak value is 1.35 times higher than the measured one, and the peak position has a shift of 0.5 mm towards the burner surface. For 1,3-butadiene, the profile shape is extremely well predicted and the peak value is only underpredicted by 17%. Compared with the experimental profile, the peak position of 1,3-butadiene is also shifted toward the burner by 0.4 mm.

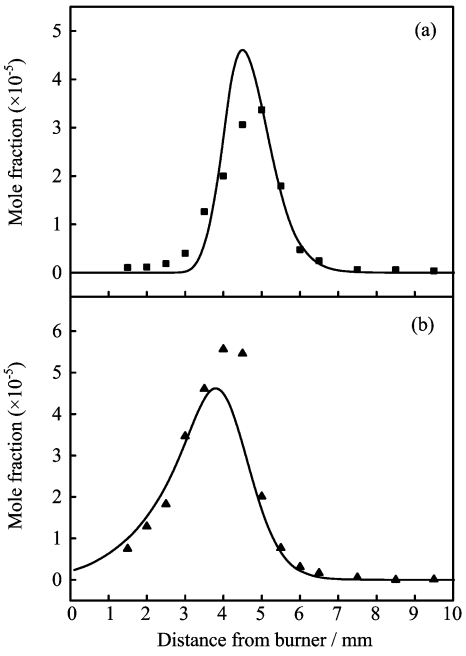

FIG. 7 Comparison between experimental mole fraction profiles (symbols) and kinetic model predictions (curves) of the propargyl radical (a) and 1,3-butadiene (b).

In this study, some new flame species are not involved in the mechanism for their inexplicit chemical properties and reaction parameters. With the development of the chemical kinetics data, thermochemistry and transport parameters, modifications to this model will be desired.

V. CONCLUSION

The experimental study of a low-pressure premixed stoichiometric ethylene flame was accomplished by using the tunable synchrotron photoionization and molecular-beam mass spectrometry techniques. Isomers of intermediates were identified with measurements of photoionization efficiency spectra by scanning the photon energy, and mole fractions were measured by scanning the burner position at selected photon energies near ionization thresholds. Compared with the studies of Bhargava and Westmoreland, a lot of new flame species were found, including unsaturated and oxygenated hydrocarbons. Precise identification of isomers extends the knowledge of ethylene flame structure and calls for further modification of current ethylene flame mechanisms. Furthermore, a reduced reaction mechanism was used for this flame. Predicted major species and intermediates profiles were also compared with the measured data. And discrepancies were analyzed theoretically.

VI. ACKNOWLEDGMENTS

This work was supported by the National Natural Science Foundation of China (No.20473081 and No.20533040), and Chinese Academy of Sciences. The authors are also thankful for the valuable help in the experimental work from Aigou Zhu. Fei Qi thanks the Combustion Research Facility of Sandia National Labs to provide a Chemkin program package for kinetic modeling study.

[1] R. D. Wilk, N. P. Cernansky, W. J. Pitz and C. K. Westbrook, Combust. Flame **77**, 145 (1989).
[2] R. P. Lindstedt and L. Q. Maurice, Combust. Sci. Technol. **107**, 317 (1995).
[3] J. Peeters and G. Mahnen, *In First European Symposium on Combustion*, England: Sheffield, 245 (1973).
[4] J. Peeters and C. Vinckier, Proc. Combust. Inst. **15**, 969 (1975).
[5] K. H. Homann, M. Mochizuki and H. G. Wagner, Z. Phys. Chem. **37**, 299 (1963).
[6] A. Bhargava and P. R. Westmoreland, Combust. Flame **115**, 456 (1998).
[7] A. Bhargava and P. R. Westmoreland, Combust. Flame **113**, 333 (1998).
[8] S. J. Harris, A. M. Weiner, R. J. Blint and J. E. M. Goldsmith, Proc. Combust. Inst. **21**, 1033 (1986).
[9] T. A. Cool, J. S. Bernstein, X. M. Song and P. M. Goodwin, Proc. Combust. Inst. **22**, 1421 (1988).
[10] R. Yang, J. Wang, C. Q. Huang, B. Yang, L. X. Wei, X. B. Shan, L. S. Sheng, Y. W. Zhang and F. Qi, Chin. Sci. Bull. **50**, 94 (2005).

ISSN 1003-7713/DOI:10.1360/cjcp2006.19(5).379.7

[11] T. A. Cool, A. M. McIlroy, F. Qi, P. R. Westmoreland, L. Poisson, D. S. Peterka and M. Ahmed, Rev. Sci. Instrum. **76**, 094102 (2005).
[12] C. K. Westbrook, F. L. Dryer and K. P. Schug, Proc. Combust. Inst. **19**, 153 (1982).
[13] M. Cathonnet, F. Gaillard, J. C. Boettner, P. Cambray, D. Karmed and J. C. Bellet, Proc. Combust. Inst. **20**, 819 (1984).
[14] R. P. Lindstedt and G. Skevis, Proc. Combust. Inst. **28**, 1801 (2000).
[15] H. Richter and J. B. Howard, Phys. Chem. Chem. Phys. **4**, 2038 (2002).
[16] T. Carriere, P. R. Westmoreland, A. Kazakov, Y. S. Stein and F. L. Dryer, Proc. Combust. Inst. **29**, 1257 (2002).
[17] F. Qi, R. Yang, B. Yang, C. Q. Huang, L. X. Wei, J. Wang, L. S. Sheng, Y. W. Zhang, Rev. Sci. Instrum. **77**, 084101 (2006).
[18] C. Q. Huang, B. Yang, R. Yang, J. Wang, L. X. Wei, X. B. Shan, L. S. Sheng, Y. W. Zhang and F. Qi, Rev. Sci. Instrum. **76**, 126108 (2005).
[19] J. H. Kent, Combust. Flame **14**, 279 (1970).
[20] M. Kamphus, N. N. Liu, B. Atakan, F. Qi and A. McIlroy, Proc. Combust. Inst. **29**, 2627 (2002).
[21] T. A. Cool, K. Nakajima, C. A. Taatjes, A. McIlroy, P. R. Westmoreland, M. E. Law and A. Morel, Proc. Combust. Inst. **30**, 1681 (2004).
[22] R. M. Fristrom, *Flame Structure and Process*, New York: Oxford, 175 (1995).
[23] A. T. Hartlieb, B. Atakan and K. Kohse-Hoinghaus, Combust. Flame **121**, 610 (2000).
[24] P. J. Linstrom and W. G. Mallard, *NIST Chemistry Webbook, NIST Standard Reference Database Number 69, Gaithersburg*, MD: National Institute of Standard and Technology, (2003). http://webbook.nist.gov.
[25] J. Warnatz, Proc. Combust. Inst. **18**, 369 (1981).
[26] V. Decottignies, L. Gasnot and J. F. Pauwels, Combust. Flame **130**, 225 (2002).
[27] C. A. Taatjes, N. Hensen, A. McIlory, J. A. Miller, J. P. Senosiain, S. J. Klippenstein, F. Qi, L. S. Sheng, Y. W. Zhang, T. A. Cool, J. Wang, P. R. Westmoreland, M. E. Law, T. Kasper and K. Kohse-Höninghaus, Science **308**, 1887 (2005).
[28] C. A. Taatjes, N. Hensen, J. A. Miller, T. A. Cool, J. Wang, P. R. Westmoreland, M. E. Law, T. Kasper and K. Kohse-Höninghaus, J. Phys. Chem. A **110**, 3254 (2006).
[29] C. J. Pope and J. A. Miller, Proc. Combust. Inst. **28**, 1519 (2000).
[30] S. E. Stein, J. A. Walker, M. M. Suryan and A. Fahr, Proc. Combust. Inst. **23**, 85 (1990).
[31] J. A. Miller and C. F. Melius, Combust. Flame **91**, 21 (1992).
[32] J. A. Miller and S. J. Klippenstein, J. Phys. Chem. A **107**, 7783 (2003).
[33] M. Frenklach, D. W. Clary, W. C. Gardiner Jr. and S. E. Stein, Proc. Combust. Inst. **20**, 887 (1984).
[34] M. E. Law, T. Carrire and P. R. Westmoreland, Proc. Combust. Inst. **30**, 1353 (2005).
[35] M. Riservato, A. Rolla and E. Davoli, Rapid Commun. Mass Spectrom. **18**, 399 (2004).
[36] J. C. Biordi, C. P. Lazzara and J. F. Papp, Combust. Flame **23**, 73 (1974).
[37] D. Stepowski, D. Pucchberty and M. J. Cottereau, Proc. Combust. Inst. **18**, 1567 (1981).
[38] R. Yang, B. Yang, C. Q. Huang, L. X. Wei, J. Wang, X. B. Shan, L. S. Sheng, Y. W. Zhang, F. Qi, C. D. Yao, Q. Li and Q. Ji, Chin J. Chem. Phys. **19**, 25 (2006).

ISSN 1003-7713/DOI:10.1360/cjcp2006.19(5).379.7